

Stabilization of continuum generation from normally dispersive nonlinear optical fibers for a tunable broad bandwidth source for optical coherence tomography

Haohua Tu, Daniel L. Marks, Yee Lin Koh, and Stephen A. Boppart*

Biophotonics Imaging Laboratory, Beckman Institute for Advanced Science and Technology, University of Illinois at Urbana-Champaign, 405 North Mathews Avenue, Urbana, Illinois 61801, USA

*Corresponding author: boppart@uiuc.edu

Received April 6, 2007; revised April 30, 2007; accepted May 14, 2007;
posted May 21, 2007 (Doc. ID 81906); published July 9, 2007

Continuum generation from normally dispersive ultrahigh-numerical-aperture fibers deteriorates in relatively short times, limiting its application as a practical optical source for high-resolution optical coherence tomography. We find that reversible light-induced structural modification of fiber optic materials, rather than permanent optical damage, is responsible for this deterioration. By examining how the optical properties of corresponding light-induced waveguides depend on pumping wavelength, we isolate a waveguide that is beneficial for stable continuum generation. The performance deterioration due to the formation of other waveguides can be reversed by overwriting them with this particular waveguide. © 2007 Optical Society of America

OCIS codes: 190.7110, 110.4500, 190.4370.

Continuum generation from photonic crystal fibers [1], tapered fibers [2], polarization-preserving fibers [3], and ultrahigh-numerical-aperture (UHNA) fibers [4] pumped by a single ultrafast oscillator is a wide-bandwidth source necessary for high-resolution optical coherence tomography (OCT). The general trend is to operate these fibers in the normal dispersion regime to promote self-phase modulation [5–7] and therefore largely suppress noisy nonlinear optical processes [8] responsible for a loss of ~15 dB in the signal-to-noise ratio [3]. We focus on UHNA fibers because they are inexpensive, readily available, and compatible with fiber optic OCT systems [4]. They have facilitated several practical OCT studies [9–12] and may dramatically improve multimodality microscope systems [13] by incorporating high-resolution OCT structural imaging (using the broadband continuum) and selective multiphoton microscopy (using the tunable narrowband oscillator output). However, the high peak pulse intensity in these fibers produces material property modifications to deteriorate the continuum generation, as discussed below. We examine the nature of this performance deterioration and develop a simple optical reversion procedure.

Two standard silica UHNA fibers (UHNA3 and UHNA4, Nufern, East Granby, Connecticut) were selected for this study. Both have a step-index-type $\text{GeO}_2\text{-SiO}_2$ core, a NA of 0.35, and a mode field diameter of $\sim 2.5 \mu\text{m}$ (at 1100 nm). The pumping source is a tunable Ti:sapphire laser (Mai Tai HP, Spectra-Physics, Mountain View, California), producing ~ 100 fs pulses with ~ 10 nm bandwidth at a repetition rate of 80 MHz. The intended operating wavelengths of UHNA3 (1300 nm) and UHNA4 (1550 nm) are much larger than the pumping wavelength so that these fibers are presumably operated in the normal dispersion regime. The laser beam of ~ 1.2 mm diameter was passed through a Faraday isolator, a

neutral-density attenuator, a 0.65 NA, 3.6 mm diameter aspheric lens, and finally coupled into a fiber. The aspheric lens and the fiber were mounted on a three-axis fiber positioner. The coupling efficiency from free space to fiber was determined by measuring the ratio of the maximized power exiting the fiber (output) to the power before entering the fiber (input) at a relatively low input (typically 50 mW), assuming that the transmission losses in the short (< 5 m) fiber length were negligible.

The high laser power allowed us to establish the damage threshold of UHNA3. The coupling efficiency was first optimized at a fixed pumping wavelength. Then the output was recorded as the input was increased, as shown in Fig. 1. The output drops to near zero when the input passes a critical value, i.e., the damage threshold. We believe the avalanche-breakdown mechanism is responsible for this observation, even though the mechanism itself suggests little wavelength dependence [14]. The observed dependence can be attributed to the wavelength dependence of the focused spot size of the aspheric lens ($\sim 1 \mu\text{m}$).

It is then somewhat surprising that the bandwidth of the continuum from UHNA3 decreases progres-

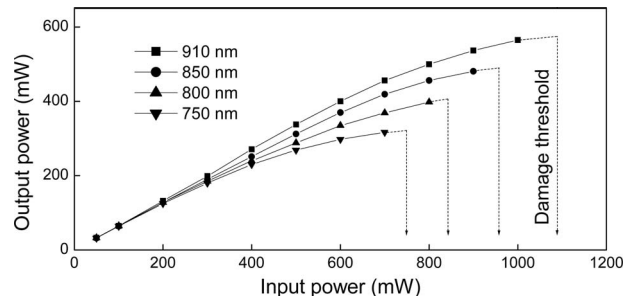


Fig. 1. Output power from a freshly cleaved UHNA3 fiber as a function of input power for several pumping wavelengths.

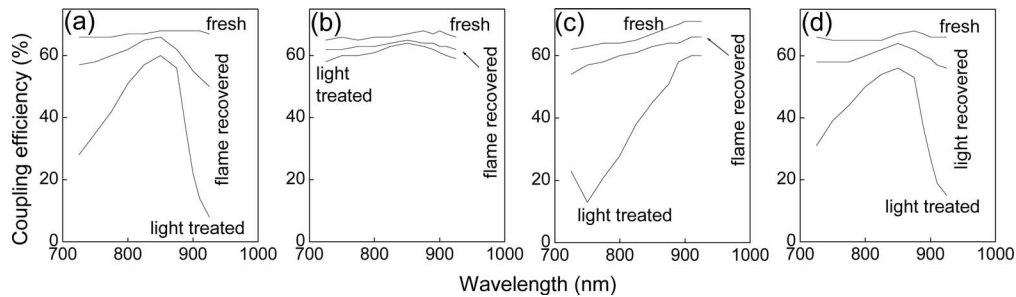


Fig. 2. (a) CES of a UHNA3 fiber when freshly prepared, light treated (800 nm, 400 mW, 1 h), and flame recovered; (b) CES of a second UHNA3 fiber when freshly prepared, light treated (910 nm, 500 mW, 8 h), and flame recovered; (c) CES of a UHNA4 fiber when freshly prepared, light treated (910 nm, 500 mW, 0.5 h), and flame recovered; (d) CES of a third UHNA3 fiber when freshly prepared, light treated (800 nm, 400 mW, 1 h), and light recovered (910 nm, 600 mW, 3 h).

sively and relatively quickly when pumped at 400 mW (800 nm), well below its damage threshold. This motivated us to compare the coupling efficiency as a function of pumping wavelength, termed the coupling efficiency spectrum (CES), before and after the deterioration. The CES of a freshly cleaved UHNA3 fiber (1–5 m) has a nearly constant value of 67% across the 725–925 nm spectral range, as shown in Fig. 2(a). The fiber was subsequently pumped at 400 mW (800 nm) with a maximized output of 230 mW. The laser source spectrum and the initial continuum spectrum are shown in Fig. 3(a). The continuum generation deteriorated 1 h later, as the FWHM of the spectrum decreased from 101 to 62 nm [Fig. 3(a)] and the output dropped by ~15%. The CES was again measured, exhibiting a dramatic filterlike profile that peaked around 850 nm [Fig. 2(a)]. The formation of this profile may be directly responsible for the observed spectrum narrowing in Fig. 3(a). A storage time of 5 days had no effect on the CES of this fiber, indicating a persistent modification. This type of modification is localized within 10 mm from the fiber entrance surface, as cleavage and removal of this length provide a new facet that behaves identically to a freshly cleaved fiber. Thus, the modification is associated with high peak pulse intensity localized at the fiber entrance due to the normal dispersion, and the modified region of the fiber core is termed the nonlinear section.

To evaluate the thermal stability of the modification, the tip of a candle flame (with a measured temperature of 1620 K) was applied to the nonlinear section of the above light-treated fiber for ~1 min, and the CES of the fiber was again measured [Fig. 2(a)]. The flame largely erased the filterlike effect. Such a flame-recovered fiber becomes susceptible to additional exposures of 800 nm radiation, just like a freshly cleaved fiber. Thus the deterioration of the continuum generation is likely due to a reversible structural modification, i.e., a waveguide structure. The benign nature and the reversibility of this modification may have prevented us from unambiguously identifying it with imaging.

Similar filterlike CESs are observed at a pumping wavelength within 750–850 nm with a wide range of power and time durations, but not at 910 nm. Figure 2(b) shows the CES of a second UHNA3 fiber (1–5 m) when freshly prepared and light treated at 500 mW

(910 nm) for 8 h. Although the CES suffers a ~10% loss, it remains flat across the observed spectral range. Further irradiation does not appreciably decrease the CES, most likely because the light–matter interaction has reached a steady state. This permits stable continuum generation with a spectrum similar to that shown in Fig. 3(b). Similarly, the flame treatment allows the CES to recover to that of a freshly cleaved fiber [Fig. 2(b)]. Thus it is likely that 910 nm irradiation also writes a waveguide in the UHNA3 fiber, but this specific waveguide happens to have a flat CES profile. As a comparison, the same experiment was conducted on a 5 m UHNA4 fiber (with core composition presumably similar to UHNA3), which shows that 910 nm irradiation generates a structured CES [Fig. 2(c)].

Since the waveguide formation is due to reversible structural modification without varying chemical composition, it is expected that the filterlike waveguide associated with 800 nm irradiation can be overwritten by the flat-CES waveguide associated with 910 nm irradiation, and vice versa. Figure 2(d) shows the CES of a third UHNA3 fiber (1–5 m) when freshly prepared and after irradiation at 400 mW (800 nm) for 1 h. The fiber developed the filterlike waveguide. This fiber was then pumped at 600 mW (910 nm) for 3 h. The maximized output was initially 130 mW, but eventually attained 340 mW. The CES of the fiber was subsequently measured, showing a flat CES profile [Fig. 2(d)]. The overwriting process can be shortened to 0.5 h if 900 mW (910 nm) of pumping power is used. The flat-CES waveguide can also be overwritten by the filterlike waveguide. For example, a fiber (1–5 m) pretreated with 910 nm irradiation (typically, at 900 mW for 1 h, or 600 mW for 3 h, or 500 mW for 8 h) requires >20 h of 400 mW (800 nm) irradiation to substantially develop the filtertype waveguide. For >4 h of operating time, the continuum generation is relatively stable, with a spectrum similar to that shown in Fig. 3(b). The presence of the flat-CES waveguide significantly slows the deterioration of the continuum generation, allowing prolonged OCT operation at a pumping wavelength of 750–850 nm. Not surprisingly, the removal of this waveguide by the flame treatment makes the fiber much more susceptible to 750–850 nm irradiation, just like a freshly cleaved fiber. Fortunately, the

deteriorated performance due to long 750–850 nm irradiation can always be reversed by another cycle of 910 nm irradiation.

A fiber (1–5 m) containing the flat-CES waveguide exhibits a continuum spectrum with a center wavelength tunable across 800–910 nm and a FWHM of >100 nm when pumped at modest input powers [Fig. 3(b)]. The nearly symmetric broadening is indicative of self-phase modulation in the normal dispersion operating regime, resulting in small sidelobes on the OCT point spread function [5]. For 910 nm operation, the continuum spectrum and output power remain stable for >40 h (in 5 days) if small laser beam drifting is compensated for by slight optical realignment. The center wavelength can be extended beyond 1000 nm if a suitable aspheric lens is chosen, as demonstrated before for a similar UHNA fiber [5]. This tunability is useful to assess the wavelength dependence of the penetration depth and imaging contrast of various tissue samples. At a given pumping wavelength, the FWHM of the continuum is also easily tunable by adjusting the pumping power, as demonstrated in Fig. 3(c).

The observed photosensitivity resembles the IR photodarkening effect widely observed in rare-earth-doped silica fibers [15]. Also, the corresponding waveguides behave similarly to the light-induced holographic gratings observed in Eu^{3+} doped glass, which are erasable either thermally or optically [16]. The photodarkening effect and the formation of the gratings have been attributed to the properties of the doped rare-earth ions. Similarly, the photosensitivity associated with the UHNA fibers is likely related to the properties of the doped Ge because germanosilicate fibers are known to have high UV photosensitiv-

ity. The TW/cm^2 -scale peak power intensity employed in this study may produce the observed IR photosensitivity in germanosilicate fibers through multiphoton processes similar to those responsible for the IR photodarkening effect.

In summary, we demonstrate that the long exposure of nanojoule femtosecond pulses from a laser oscillator produces various waveguides at the entrance of a germanosilicate fiber below its damage threshold, causing the deterioration of the continuum generation. By optimizing the pumping wavelength, we find a specific waveguide that is beneficial for creating a stable center-wavelength-tunable broadband sources for OCT. Utilizing the rewritable capability of the undamaged fiber optic materials (i.e., the reversibility of the waveguide formation), we reverse this deterioration by preferentially writing this waveguide.

This work was supported in part by grants from the National Science Foundation (Office of Basic Energy Science 03-47747 and 06-19257, S.A.B.) and from the National Institutes of Health (Roadmap Initiative 1 R21 EB005321, and NIBIB 1 R01 EB005221, S.A.B.).

References

1. J. K. Ranka, R. S. Windeler, and A. J. Stentz, *Opt. Lett.* **25**, 25 (2000).
2. T. A. Birks, W. J. Wadsworth, and P. S. J. Russell, *Opt. Lett.* **25**, 1415 (2000).
3. Y. Wang, I. Tomov, J. S. Nelson, Z. Chen, H. Lim, and F. Wise, *J. Opt. Soc. Am. A* **22**, 1492 (2005).
4. D. L. Marks, A. L. Oldenburg, J. J. Reynolds, and S. A. Boppert, *Opt. Lett.* **27**, 2010 (2002).
5. S. Bourquin, A. D. Aguirre, I. Hartl, P. Hsiung, T. H. Ko, J. G. Fujimoto, T. A. Birks, W. J. Wadsworth, U. Bunting, and D. Kopf, *Opt. Express* **11**, 3290 (2003).
6. N. Nishizawa, Y. Chen, P. Hsiung, E. P. Ippen, and J. G. Fujimoto, *Opt. Lett.* **29**, 2846 (2004).
7. G. Humbert, W. Wadsworth, S. Leon-Saval, J. Knight, T. Birks, P. St. J. Russell, M. Lederer, D. Kopf, K. Wiesauer, E. Breuer, and D. Stifter, *Opt. Express* **14**, 1596 (2006).
8. K. L. Corwin, N. R. Newbury, J. M. Dudley, S. Coen, S. A. Diddams, K. Weber, and R. S. Windeler, *Phys. Rev. Lett.* **90**, 113904 (2003).
9. M. Lazebnik, D. L. Marks, K. Potgieter, R. Gillette, and S. A. Boppert, *Opt. Lett.* **28**, 1218 (2003).
10. T. M. Lee, F. J. Toublan, S. Sitafalwalla, A. L. Oldenburg, K. S. Suslick, and S. A. Boppert, *Opt. Lett.* **28**, 1546 (2003).
11. C. Xu, J. Ye, D. L. Marks, and S. A. Boppert, *Opt. Lett.* **29**, 1647 (2004).
12. W. Tan, A. L. Oldenburg, J. J. Norman, T. A. Desai, and S. A. Boppert, *Opt. Express* **14**, 7159 (2006).
13. C. Vinegoni, T. Ralston, W. Tan, W. Luo, D. L. Marks, and S. A. Boppert, *Appl. Phys. Lett.* **88**, 053901 (2006).
14. R. W. Boyd, *Nonlinear Optics* (Academic, 2003).
15. J. J. Koponen, M. J. Söderlund, H. J. Hoffman, and S. K. Tammela, *Opt. Express* **14**, 11539 (2006).
16. E. G. Behrens, F. M. Durville, and R. C. Powell, *Opt. Lett.* **11**, 653 (1986).

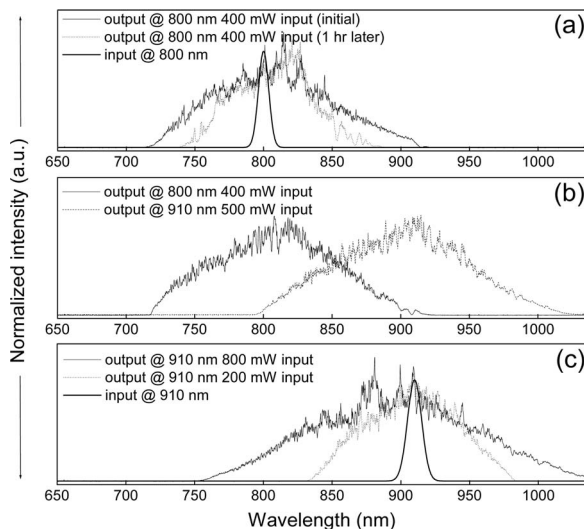


Fig. 3. (a) Comparison of the input and output spectrum from a freshly prepared UHNA3 fiber and the output spectrum after light treatment (800 nm, 400 mW, 1 h); (b) broadband continuum generation from a light-pretreated (910 nm, 900 mW, 1 h) UHNA3 fiber with tunable center wavelength across 800–910 nm; (c) continuum generation from the light-pretreated fiber with bandwidth tunable by adjusting the input power.